Photoelectrochemical hydrogen production by water splitting over dual-functionally modified oxide: p-Type N-doped Ta_2O_5 photocathode active under visible light irradiation

Tomiko M. Suzuki*, Shu Saeki, Keita Sekizawa, Kosuke Kitazumi, Naoko Takahashi, Takeshi Morikawa*

Toyota Central R&D Labs. Inc., 41-1, Yokomichi, Nagakute, Aichi, 480-1192, Japan

ARTICLE INFO

ABSTRACT

Doping of nitrogen into tantalum pentoxide (Ta_2O_5) drastically modifies two semiconductor characteristics simultaneously; first is activation toward visible light region from 320 to 520 nm in wavelength and second is reversed polarity in photoresponse from n-type to p-type conduction. N-doped Ta_2O_5 (N-Ta_2O_5) was also found to possess highly negative energy position of conduction band minimum (-1.3 V vs NHE) compared to those of Ta_2O_5 and TaON (-0.3 V), which was originated from surface dipole effect as recently clarified by DFT calculation reported in a literature. Here, we exhibit the first demonstration of photoreaction over N-Ta_2O_5 in an aqueous solution. The surface of N-Ta_2O_5 was found to be almost inert for hydrogen production by water splitting. However, the hydrogen generation rate was highly enhanced by surface modification with Pt, Rh or Au, which was assessed by photocathodic current over N-Ta_2O_5 films under visible light irradiation ($\lambda \geq 410$ nm). Among them, loading with either Pt or Rh greatly enhanced the H_2 evolution rate in an aqueous solution by two orders of magnitude compared to that over unmodified N-Ta_2O_5 for both films and powders. These results imply that the dual functional modification by single doping of N has a potential to generate new photocathodes for water splitting reaction under visible light irradiation.

© 2016 Elsevier B.V. All rights reserved.

1. Introduction

It is widely accepted that photocatalytic hydrogen generation by water splitting and carbon dioxide recycling by reductive reaction are promising technologies as clean energy generation in the future. To this end, lots of semiconductor materials which can be activated under visible light irradiation have been developed to date. To realize the reactions, position of conduction band minimum of semiconductors is primarily important to facilitate conduction band electrons to protons, CO_2 molecules, and cocatalysts, which should be located to be much more negative than that of normal hydrogen electrode (NHE). Recently, our group developed an N-doped Ta_2O_5 (N-Ta_2O_5) that absorbs visible light at wavelengths below 520 nm ($Eg = 2.4$ eV) by forming a new energy state in which the N $2p$ is above the O $2p$ in the bandgap [1,2]. The N-doping also changed its photoresponse from anodic to cathodic probably due

to formation of acceptor level by N, and also resulted in a highly negative location of the conduction band minimum ($E_{CBM} = -1.3$ V vs NHE) [1,2]. However, it is important these characters as a semiconductor are completely different from those of conventional tantalum pentoxide (Ta_2O_5, $Eg = 4.0$ eV, $E_{CBM} = -0.4$ V vs NHE) [3–6] and tantalum oxynitride (TaON, $Eg = 2.4$ eV, $E_{CBM} = -0.3$ V vs NHE) [6], which exhibit anodic photoresponses. Depending on the much negative E_{CBM}, a highly selective visible light-induced reduction of CO_2 to HOOH was achieved by employing powdered N-Ta_2O_5 linked with a ruthenium complex catalyst in acetonitrile (MeCN)/triethanolamine (TEOA) [7,8]. This work demonstrated that an important factor in the activity was the ultrafast electron transfer from the N-Ta_2O_5 in its photoexcited state to the Ru complex (12 ± 1 ps), the speed of which exceeded that of the carrier trapping processes in N-Ta_2O_5 (24 ± 1 ps) [9], and a theoretical approach clarified electronic interaction between semiconductors and complexes was also essential to the electron transfer [10]. Based on these prior results, the development of p-type oxide semiconductors having both highly negative E_{CBM} values and an enhanced response to visible light appears promising for the energy-storage or reductive reactions. It is thus worthwhile to

assess such materials with regard to utilization as photocathodes for reductive reactions of water or CO_2 to produce useful chemicals such as hydrogen and hydrocarbons. However, to date, only a limited number of *p*-type oxide semiconductor photocathodes have been reported, including Cu_2O [11,12], $CuNb_3O_8$ [13], Rh-doped $SrTiO_3$ [14], metal-doped Fe_2O_3 [15,16], N-doped Fe_2O_3 [17,18], $CaFe_2O_4$ [19,20] and Ag-doped $CaFe_2O_4$ [21]. Moreover, there are few reports concerning H_2 production utilizing *p*-type oxide photocathodes under visible light irradiation [13–16,20]. Challenges to find new semiconductor materials for photocathodes are necessary. In this paper, we demonstrate for the first time the potential of $N-Ta_2O_5$ showing a *p*-type photoresponse as a visible light sensitive photocathode for hydrogen production by water splitting. Because crystallinity is poor at this moment depending on present synthesizing method, overall activities are low. However, this paper suggests a new methodology for realizing new materials by the anionic doping in oxides for the dual–functional modification.

2. Experimental

2.1. Materials

$N-Ta_2O_5$ films were deposited onto antimony-doped tin oxide (ATO)-coated glass substrates by sputtering of Ta_2O_5 using a plasma generated from a N_2/Ar gas mixture (20×20 mm^2), followed by annealing at 873 K under a N_2 gas flow, employing a method reported previously [1]. Various metals (Pt, Au, Rh, Ir, Ru and Ni) intended as H_2 evolution cocatalysts were subsequently sputtered onto the surface of the $N-Ta_2O_5$ films or a transparent conductive oxide film (SnO_2-ITO, Geomatech) at a nominal thickness of 1 nm, as calculated from the deposition rates.

Powdered $N-Ta_2O_5$ as references were synthesized by annealing Ta_2O_5, prepared using $TaCl_5$ and aqueous ammonia, under an NH_3 flow at 848 K for 6 h according to a previously reported method [1]. Powdered TaON and Ta_3N_5 were also prepared by annealing Ta_2O_5 under an NH_3 for 6 h, at 1093 K and 1123 K, respectively. Metal cocatalysts (*ca.* 0.5 wt%) were loaded on the $N-Ta_2O_5$ particles by photodeposition in triethanolamine (10 vol.%)-methanol mixed solutions which contained metal-precursors. In the case of TaON and Ta_3N_5 particles, the photodeposition was performed in 80 vol% methanol aqueous solution which contained various metal-precursors [11].

3. Structural characterization

Chemical states and concentrations of N doped in Ta_2O_5 and cocatalysts were determined by X-ray photoelectron spectroscopy (XPS; PHI-5500MC, ULVAC-PHI) using monochromated Al Kα radiation. Crystal structure was measured by an X-ray diffractometer (Ultima IV, Rigaku) using Cu Kα radiation at 40 kV and 40 mA. Photoelectron spectroscopy in air (PESA) was performed with an AC-2 photoelectron spectrometer (Riken-Keiki Co., Ltd.) and UV–vis diffuse reflectance spectra were acquired using a UV-3600 spectrometer (Shimadzu).

3.1. Basic photoelectrochemical measurements

The photoelectrochemical characteristics of $N-Ta_2O_5$ films were investigated in an aqueous 0.2 M K_2SO_4 solution according to a previous report on $SrTiO_3$:Rh showing a noble cathodic photoresponse for hydrogen generation [14]. A three-electrode configuration using a Ag/AgCl reference electrode and a Pt wire counter electrode was employed. Photoelectrochemical cells containing 0.2 M K_2SO_4 and photoelectorodes were purged with Ar gas and irradiated with visible light (300W Xe lamp <MAX-303, Asahi Spectra> with 42L

filter, $\lambda \geq 410$ nm, 99.99%-cut-off). The light intensity was adjusted at 45 mW/cm^2 using a power meter (C9536-01, Hamamatsu Photonics) in the absence of the 42L cutoff filter, and samples area of 1 cm^2 were irradiated. The wavelength dependence of the incident photon to current efficiency (IPCE) [22] was determined under monochromatic irradiation from the Xe lamp equipped with band-pass filters (central wavelengths ranging 360–600 nm with 20 nm steps).

3.2. Photoelectrochemical hydrogen evolution by water splitting

Photoelectrochemical H_2 evolution of $N-Ta_2O_5$ films were investigated using a Pyrex sealed glass reactor (total volume: 118.9 ml) in an aqueous 0.2 M K_2SO_4 solution at pH 5.8 (50 ml), according to a previous report on $SrTiO_3$:Rh [14]. A three-electrode configuration using a Ag/AgCl reference electrode and a Pt wire counter electrode was employed and applied potential was set at −0.4 V. Intensity of the Xe lamp (with 42L, $\lambda \geq 410$ nm) was adjusted at 110 mW/cm^2. Amounts of H_2 photogenerated by water splitting over the $N-Ta_2O_5$ photocathodes were determined using a gas chromatograph equipped with a TCD detector (GC-2014, Shimadzu).

3.3. Photocatalytic hydrogen evolution using Ta-based semiconductor particles

Photocatalytic activity was measured at ambient pressure in 8 ml sealed test tubes containing 4 ml an aqueous solution with a 100 mM electron donor or 80 vol% methanol aqueous solution and 8 mg photocatalyst. The chemicals used as electron donor were L(+)-ascorbic acid (Wako, 99.6%) and ethylenediamine-N,N,N',N'-tetraacetic acid disodium salt dehydrate (EDTA: Wako, 99.5%). pH adjustment of 100 mM EDTA aqueous solution was performed by utilization of NaOH aqueous solution. After purging with Ar for 15 min, the solutions were irradiated using a 500 W Xe lamp with a band-pass filter to produce light in the range $390 \leq \lambda \leq 750$ nm. The systems were irradiated for 24 h at room temperature, and product concentrations were determined by gas chromatography.

4. Results and discussion

4.1. Crystalline and electronic band structure of $N-Ta_2O_5$ films

In previous literatures, it was reported that $N-Ta_2O_5$ powder possessed orthorhombic structure and large amount of N (>5at.%) was doped in the crystalline [1,2,7]. As shown in Fig. 1a, the XRD pattern of $N-Ta_2O_5$ (b) was similar to that of non-doped Ta_2O_5 (a) and very broad peaks at around $2\theta = 35°$ were also observed, which indicated a low level of preferred crystalline orientation in the film. These results indicate that N doping does not affect the crystal structure of Ta_2O_5. Because broad peak was also detected in the case of Si (100) substrate (c), it was speculated that the peak arose from crystalline phase of Ta_2O_5. We inserted reference data of Ta_2O_5 crystal (PDF#01-073-2323) at the bottom of Fig. 1a. However, owing to its low crystallinity, it is difficult to determine the crystal structure. To obtain sharp peaks, heat treatment at higher temperature (750–800 °C) is needed. At this moment, the annealing temperature is limited less than 600 °C, which is dependent on heat resistance of ATO substrate and condition for avoiding N elimination from the sputtered $N-Ta_2O_5$. We have also conducted cross-sectional TEM observation of $N-Ta_2O_5$ sample, which indicated that nanoscale $N-Ta_2O_5$ particles were highly dispersed in amorphous phase (Figs. S1 and 2). These results are consistent with the XRD, which explains that nanocrystalline $N-Ta_2O_5$ were highly dispersed in amorphous phase. However, because there is a possibility the nanoparticles confirmed by the TEM observation might be formed during focused ion beam (FIB) milling for preparing TEM
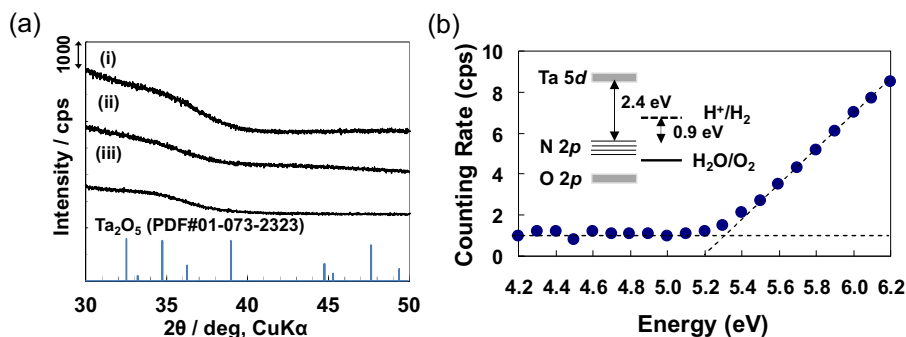
Fig. 1. (a) XRD patterns of (i) Ta_2O_5 film on glass substrate, (ii) N-Ta_2O_5 film on glass substrate and (iii) N-Ta_2O_5 film on Si substrate. (b) PESA spectrum of N-Ta_2O_5 film. The inset shows a band diagram for N-Ta_2O_5 together with the potentials for hydrogen and oxygen generation by water splitting.
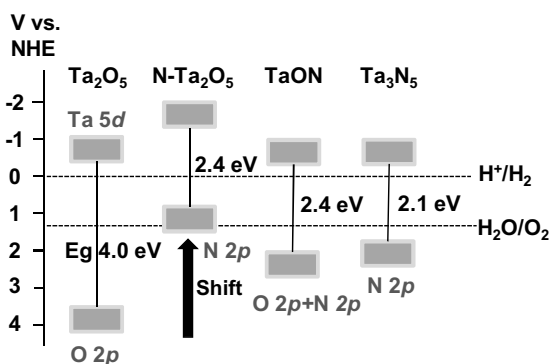

Fig. 2. Schematic illustration of band structures of various Ta-based semiconductors. The band positions of Ta_2O_5, TaON and Ta_3N_5 were adopted from Refs. [4] and [6].

specimen or TEM observation under high energy, it is difficult to conclude the existence of nanocrystalline in amorphous-rich Ta_2O_5 and N-Ta_2O_5 phase.

The nitrogen concentration of the films was estimated to be 7.6at% by XPS analysis, and the results were found to be in good agreement with previously reported values [1]. N-Ta_2O_5 is neither oxynitride nor solid solution of oxide and nitride. Doping of N into oxides induces new states like substitutional N (N^{3-}), substitutional NO_2, interstitial NO, oxygen vacancy, etc. in the bandgap, which has been discussed on TiO_2, a well-known oxide catalyst [23,24]. Furthermore, N can cause *p*-type conductivity [25,26] depending on the N state, because it is generally accepted that atomic N forms an acceptor level in oxide band gaps, resulting in hole generation. Based on the facts, it was postulated for the N-Ta_2O_5 that the broad peak around 400 eV was responsible for the sensitivity to visible light and that the peak at 396.6 eV was mainly responsible for the *p*-type conduction [1]. N-Ta_2O_5 is known to show reductive reaction of CO_2 [7] under N $2p \rightarrow$ Ta $5d$ photoexcitation by visible photons.

From the PESA data provided in Fig. 1b, the ionization potential (IP) of the N-Ta_2O_5 film was estimated to be 5.32 eV, indicating that nitrogen doping resulted in a significant negative shift in the IP of the original Ta_2O_5 which is approximately 7.9 eV. As shown in Fig. 2, the IP was calculated to be +0.9 V *vs.* NHE, which explains that N-Ta_2O_5 was not able to photo-oxidize water without applying external bias voltage because E_{VBM} is located at more negative potential than that for the water oxidation (+1.23 V *vs* NHE). The E_{CBM} of Ta_2O_5 is highly negative (-1.3 V *vs.* NHE) [4], which is sufficient to produce hydrogen. In contrast, it has been reported that the conduction band minimum (E_{CBM}) of *n*-type TaON and Ta_3N_5 are close to that of *n*-type Ta_2O_5 [6]. The negative shift in the band position (CBM and VBM) induced by the N-doping in Ta_2O_5 seems unreasonable from a standpoint of solid-state physics. However,
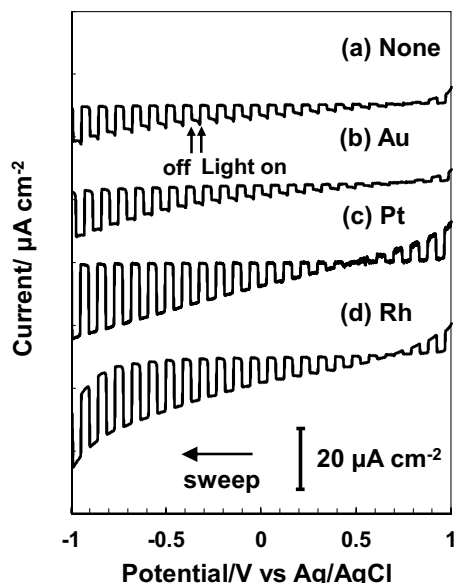

Fig. 3. Photocurrent-voltage curves of unloaded and cocatalyst loaded N-Ta_2O_5 films. These data were acquired in an aqueous 0.2 M K_2SO_4 solution under chopped visible light irradiation ($\lambda \geq 410$ nm).

recently, DFT calculations by Jinnouchi et al. revealed that surface electronic state induced by doping of N caused significantly negative shift in band-position of N-Ta_2O_5. They showed that the CB edge is shifted toward more negative energies, in which the atomistic origin of such shift was attributed to electrostatic effects due to the dipole created by the N−O layer in the doped material [27]. In XPS for Pt/N-Ta_2O_5 or Au/N-Ta_2O_5 samples, metallic Pt or Au were observed, but both metallic and oxidized noble metals were observed in the case of Rh/N-Ta_2O_5 samples (Fig. S3).

4.2. Photoelectrochemical properties of N-Ta_2O_5 films

Photoelectrochemical measurements were performed to investigate the effect of the cocatalyst on the N-Ta_2O_5 films. Fig. 3 shows photocurrent-voltage curves obtained from trials using unloaded and cocatalyst loaded N-Ta_2O_5 films, in which clear cathodic photocurrent was observed under visible light irradiation. As explained, N in the Ta_2O_5 induces dual functions, change in two semiconductor characteristics such as activation in the visible light region from 320 to 520 nm and change in the conduction from *n*-type a *p*-type photoresponse. Hence clear cathodic photocurrent was observed under visible light irradiation by photoexcitation from N $2p$ to Ta $5d$, which is completely different from the anodic photocurrent under UV irradiation by photoexcitation from O $2p$ to
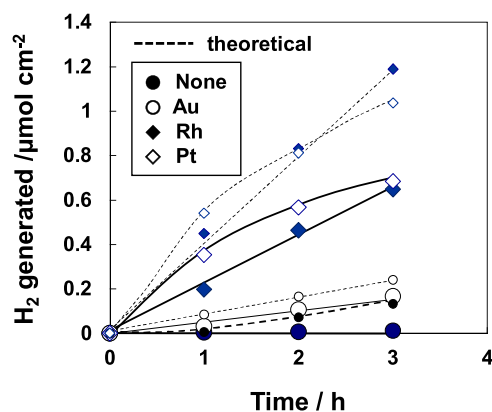
Fig. 4. H_2 evolution by photoelectrochemical water splitting over $N-Ta_2O_5$ films loaded with Pt, Rh and Au as cocatalysts over varying time spans. The applied potential was maintained at -0.4 V *vs.* Ag/AgCl and H_2 in the reactor headspace was measured ($\lambda \geq 410$ nm, in an aqueous 0.2 M K_2SO_4 solution). Theoretical curves were calculated assuming 100% Faradaic efficiency, in which smaller symbols show calculated values at the points for experimental measurements.

Table 1
Photoelectrocatalytic H_2 evolution activity of various $N-Ta_2O_5$ photocathodes measured in 0.2 M K_2SO_4 aqueous solution ($\lambda \geq 410$ nm, -0.4 V *vs.* Ag/AgCl).

Co-catalyst	Rate of H_2 evolution (nmol/h)	Faradaic efficiency (%, 3 h)	Turnover number (per metal, 3 h)
None	2	8	–
Au	53	69	169
Pt	283	66	622
Rh	231	55	537

Ta 5d [1]. However, low anodic photocurrent was also observed in Fig. 3. Because pristine Ta_2O_5 cannot be activated by visible light, it is speculated the anodic photocurrent is generated from smaller amount of other compounds showing the anodic photocurrrent such as $N-Ta_2O_5$ with lower N concentration (N content:<5at%) [1] or n-type TaON. In order to confirm the nature of $N-Ta_2O_5$, Mott-Schottky analysis was also conducted. The negative slopes which indicate p-type behavior of $N-Ta_2O_5$ were confirmed, which show a flatband potential of $+1.55$ V (*vs.* Ag/AgCl) (Fig. S4). As for the discrepancy between the flatband and onset potentials (Fig. 3), it is speculated that the overlap of the anodic photoresponse induced the negative shift of the onset potential as shown in Fig. 3.

The photocurrent was evidently enhanced by surface loading with Pt and Rh, but exhibited only minimal change following the addition of Au. In contrast, modification with Ir, Ru or Ni deteriorated the cathodic photocurrent (data not shown). Following loading with Pt and Rh, the photocurrent was increased by factors of 2.8 and 3.2 times compared to the unmodified $N-Ta_2O_5$ film, respectively (at -0.4 V *vs.* Ag/AgCl). These results indicate that surface modification with an optimal cocatalyst improves the cathodic photocurrent of the $N-Ta_2O_5$ film, which is speculated to be due to enhanced reductive reaction at the cocatalysts.

Photoelectrochemical H_2 evolution over the $N-Ta_2O_5$ films by water splitting under visible light irradiation was evaluated by one of the conventional methods using a sealed glass reactor filled with 0.2 M K_2SO_4 aqueous solution. The applied potential was set at -0.4 V *vs.* Ag/AgCl, which was close to E_{CBM} of TiO_2, $SrTiO_3$, TaON, Ta_3N_5, etc., taking into account a future coupling with these photoanode for H_2O photooxidation [28]. Since $N-Ta_2O_5$ was used as photocathodes and Pt was used for anode, it was strongly suggested that electrons for the H_2 generation was originated from species in solution at the present experimental condition. Fig. 4 presents the extents of H_2 evolution over $N-Ta_2O_5$ films loaded with Au, Pt or Rh cocatalysts as functions of time, and Table 1 summarizes the data. These results demonstrate that unmodified $N-Ta_2O_5$ generates a small amount of H_2 with low Faradaic efficiency (8%), which shows surface of $N-Ta_2O_5$ is almost inert for proton reduction reaction. As well-known photocatalsysts consisting of Ta, O, and N for hydrogen generation by water splitting, TaON and Ta_3N_5 are also known to be almost inert in the absence of cocatalysts, and reaction rates were reported to be highly improved by loading of cocatalyst [29,30]. Accordingly, in the case of $N-Ta_2O_5$ photocathode, the H_2 evolution rates were also increased by loading of cocatalysts. The factors of improvement were counted to be 27, 142 and 116

upon loading with Au, Pt and Rh, respectively, and the associated Faradaic efficiencies were enhanced by 69, 66 and 55%, respectively. The $Rh/N-Ta_2O_5$ film was found to be the most favorable photocathode with regard to stability. Photocurrent-voltage curves of unloaded and cocatalyst-loaded $N-Ta_2O_5$ films were evaluated before and after (3 h) photoelectrochemical reaction (Fig. S5). In the case of bare $N-Ta_2O_5$ possessing extremely low H_2 evolution rate and Faradaic efficiency, profile of the photocurrent-voltage curves largely changed after photoelectrochemical reaction and enhancement of dark current together with a spike-like photoresponse was observed, which was considered to be due to self-reduction by photoexited electrons. As for the Au- or Rh- loaded sample showing stable photoelectrochemical H_2 evolution activity, these photocurrent-voltage curves showed almost no change in their profiles. To the contrary, in the case of Pt loaded $N-Ta_2O_5$ films exhibiting high H_2 evolution activity and low stability, the profile largely changed after photoelectrochemical reaction, resulting in declination of photocathodic current and increase in dark current. The reason for the low stability is considered to be due to self-reduction by photoexited electrons and/or N elimination from $N-Ta_2O_5$. As for dependence of the applied bias voltage, it was also confirmed that increase in the applied voltage from -0.4 to -1.0 V significantly improved both the H_2 evolution rate (from 53 to 265 nmol/h) and the Faradaic efficiency (from 69 to 99%) of the Au-based film (Table S1). This enhancement was due to improved electron transfer from the $N-Ta_2O_5$ in the photoexcited state to the Au cocatalyst resulting in a proton reduction reaction, suggesting that the electron transfer rate from $N-Ta_2O_5$ to Au catalyst is rather insufficient even at -0.4 V.

The low Faradaic efficiency and the gradual activity degradation during the operation are speculated to be mainly due to a deteriorated $N-Ta_2O_5$ performance. To evaluate changes in chemical state of the $N-Ta_2O_5$ after the photoelectrochemical reaction, the Ta 4f binding energies for the photocathodes were investigated by XPS. We did not perform any surface cleaning or ionic etching before the XPS measurement since it may cause unfavorable reactions and damages at the surface. After background subtraction from XPS spectra using a straight-line, peak decomposition into two components were performed: one is pentavalent Ta ions Ta^{5+} and the other is more negative than Ta^{5+} (defined as "negatively-charged Ta^{5+}"), in which negatively-charged Ta^{5+} has already been reported in previous literature [1]. Only in the case of $Pt/N-Ta_2O_5$, a Ta ion species with higher valence than Ta^{5+} was observed, and it was denoted as an unassignable component (Fig. S6). Fig. 5 and Fig. S6 show XPS spectra of Ta $4f_{5/2}$ and Ta $4f_{7/2}$ for various $N-Ta_2O_5$ photocathodes before and after photoelectrochemical reaction at -0.4 V for 3 h. The results are summarized in Table 2. After the photoelectrochemical reactions, intensity of the negatively-charged Ta^{5+} was enhanced, suggesting a self-reduction of Ta^{5+} by photoexcited conduction band electrons during cathodic operation of $N-Ta_2O_5$. As-synthesized $N-Ta_2O_5$ also contained some quantity of negatively-charged Ta^{5+} (1.6–1.9%), because the heavy N doping of Ta_2O_5 causes oxygen vacancy etc. donating electrons to Ta ions to maintain a charge balance [1]. At an initial stage, existence of certain amount of Ta^{4+} is significant to realize a p-type pho-
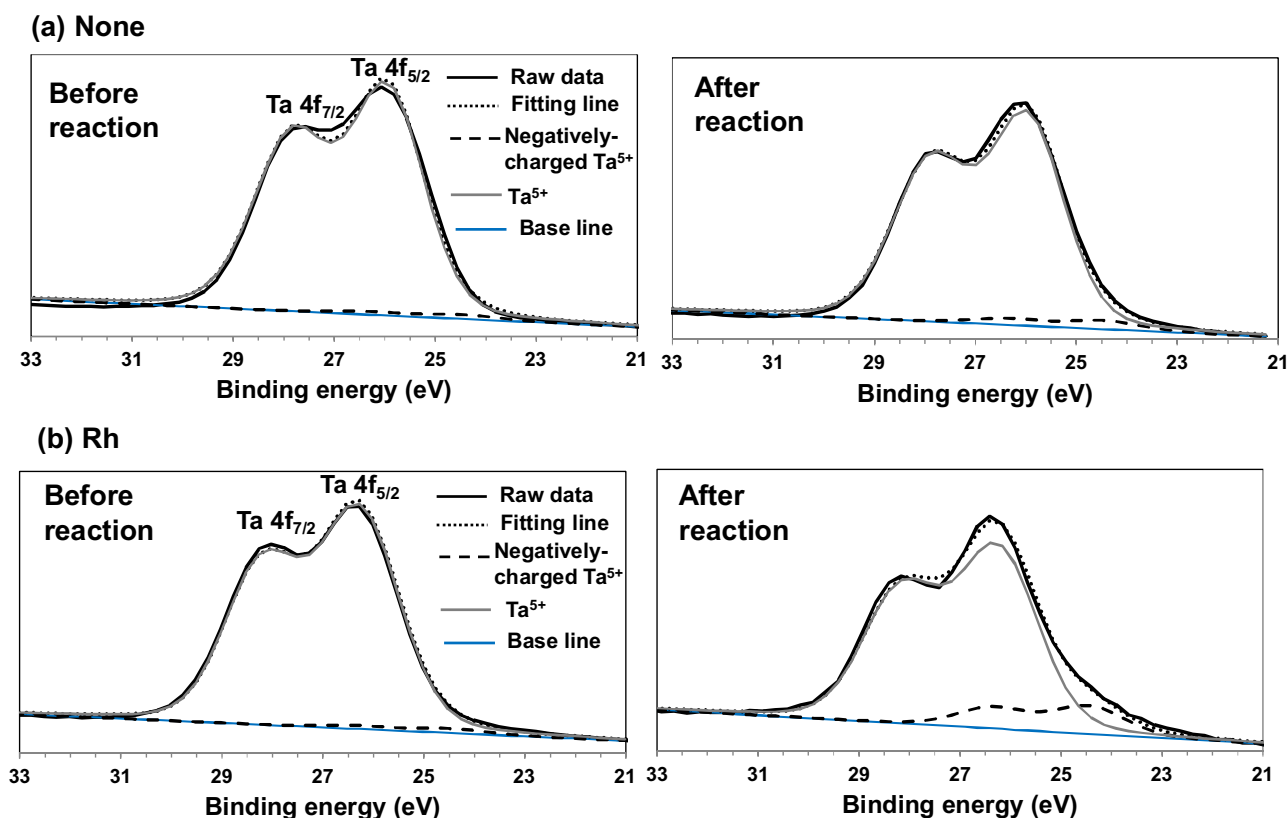
Fig. 5. XPS spectra of Ta 4*f* states for (a) unloaded N-Ta$_2$O$_5$ and (b) Rh loaded N-Ta$_2$O$_5$ before and after photocathodic reaction for 3 h at −0.4 V *vs.* Ag/AgCl.

Table 2
Reduction of Ta ions after photocathodic reaction evaluated by peak decomposition of XPS for various N-Ta$_2$O$_5$ photocathodes.

Cocatalyst	Rate of negatively-charged Ta^{5+} (%)[a]		Rate of increase of negatively-charged Ta^{5+} by photoelectrochemical reaction (%)
	Before reaction	After reaction (3 h)	
None	1.7	3.8	2.2
Pt	1.6	13.9[b]	8.7
Rh	1.9	12.6	6.6
Au	1.7	2.0	1.2

[a] Ration of (Ta ions negative than Ta^{5+}/total Ta ions).
[b] Deducted from unknown component as shown in Fig. S6 (b).

Table 3
Photocatalytic activities for hydrogen evolution over cocatalyst-loaded various Ta-based semiconductor particles in 80 vol% methanol and 100 mM EDTA aqueous solution measured under visible-light irradiation[a].

Photocatalyst	Cocatalyst (wt%)[b]	Amount of H$_2$ evolved (μmol)	
		80 vol% methanol (4 h)	100 mM EDTA(pH 4.4, 24 h)
N-Ta$_2$O$_5$	–	0.01	0.20
N-Ta$_2$O$_5$	Pt (0.30)	0.19	5.12
N-Ta$_2$O$_5$	Ru (0.47)	0.02	0.33
N-Ta$_2$O$_5$	Au(0.57)	0.00	2.22
N-Ta$_2$O$_5$	Rh (0.50)[c]	0.02	2.02
TaON	–	0.00	1.02
TaON	Pt (0.39)	0.17	3.73
TaON	Ru (0.08)	0.59	0.70
TaON	Ru(0.39)	0.33	0.01
Ta$_3$N$_5$	–	0.01	0.00
Ta$_3$N$_5$	Pt (0.19)	0.16	0.41
Ta$_3$N$_5$	Ru (0.12)	0.02	0.01

[a] Reaction condition: 8 mg catalyst in 4 ml Ar-saturated 80 vol% methanol aqueous solution at ambient temperature. Suspensions were irradiated using a 500 W Xe lamp with filters to produce light in the range 390 ≤ λ ≤ 750 nm for 4 h.
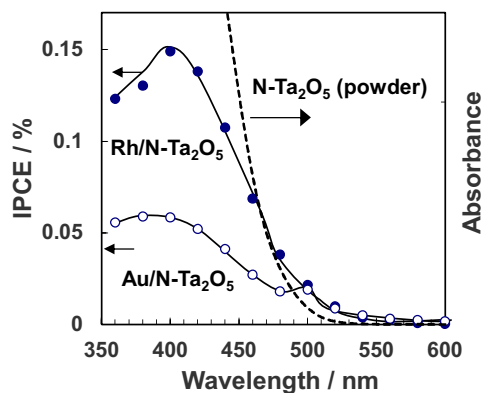[b] Estimated by ICP analysis.
[c] Calculated from amount of Rh-salt.

Fig. 6. IPCE spectra acquired at −0.4 V *vs.* Ag/AgCl together with the diffuse reflectance absorption spectrum of a N-Ta$_2$O$_5$ powder for comparison purposes.

toresponse under visible light irradiation by the dual-functional modification by doping of N. It is obvious that the increase in the negatively-charged Ta^{5+} after the photoelectrochemical reaction depended on the kind of co-catalyst. The variation in the amount of the reduction from Ta^{5+} to negatively-charged Ta^{5+} is presumably due to difference in efficiency in electron transfer from the surface of N-Ta$_2$O$_5$ to the cocatalysts and difference in reduction reaction (ability to transfer to protons to form hydrogen molecules) on the cocatalysts. N-Ta$_2$O$_5$ films loaded with Rh or Pt cocatalyst showing high hydrogen production rates were significantly self-reduced by photoexcited electrons after the 3 h operation. In contrast, comparing unmodified N-Ta$_2$O$_5$ film with Au loaded N-Ta$_2$O$_5$ films which showed lower rates than those for Pt or Rh loading, Au loading led to prevention of the self-reduction while promoting H$^+$ reduction. These results indicate that higher H$_2$ generation rate accompanies higher self-reduction of N-Ta$_2$O$_5$ at the condition of low Faradaic efficiency (55–69%), which is probably due to larger charge flow at cocatalyst-semiconductor interface facilitated by fast proton reaction to produce hydrogen at the cocatalyst surface. Further increase in the negatively-charged Ta^{5+} by the self-reduction should be decreased, which could enhance stability of photoreaction to produce hydrogen.

4.3. IPCE spectra of N-Ta$_2$O$_5$ photocathodes

IPCE data were subsequently obtained, as shown in Fig. 6. Since it was not possible to obtain a suitable absorption spectrum of the N-Ta$_2$O$_5$ films owing to the presence of a significant interference wave caused by the high dielectric constant of the material, a diffuse reflectance spectrum of a N-Ta$_2$O$_5$ powder has instead been included in this figure as a reference. Prior to the experiment, it was also confirmed that the N-Ta$_2$O$_5$ powder loaded with Pt or Au cocatalysts exhibited visible-light-induced H$_2$ production in an aqueous solution with a 100 mM electron donor (ascorbic acid or ethylenediamine-N,N,N',N'-tetraacetic acid disodium salt (EDTA)) (Table S2). Though N-Ta$_2$O$_5$ cannot oxidize water because the E$_{VBM}$ is positioned to be more negative than H$_2$O oxidation potential, hydrogen generation can be realized by supplying other sacrificial electron donor molecules, which will be explained later.

In the photoelectrochemical system using the N-Ta$_2$O$_5$ electrode, it is evident that the wavelength dependencies of the IPCE values of the Au/N-Ta$_2$O$_5$ and Rh/N-Ta$_2$O$_5$ films, both of which produce H$_2$ under visible light illumination less than 550 nm, are almost coincident with the photoabsorption profile. The IPCE values at 400 nm for Rh/N-Ta$_2$O$_5$ and Au/N-Ta$_2$O$_5$ were 0.15 and 0.06%, respectively, and thus the use of Rh, which also gave a higher rate of H$_2$ evolution, appears to generate the greatest level of enhancement. Because N-Ta$_2$O$_5$ films having a low level of crystallinity will

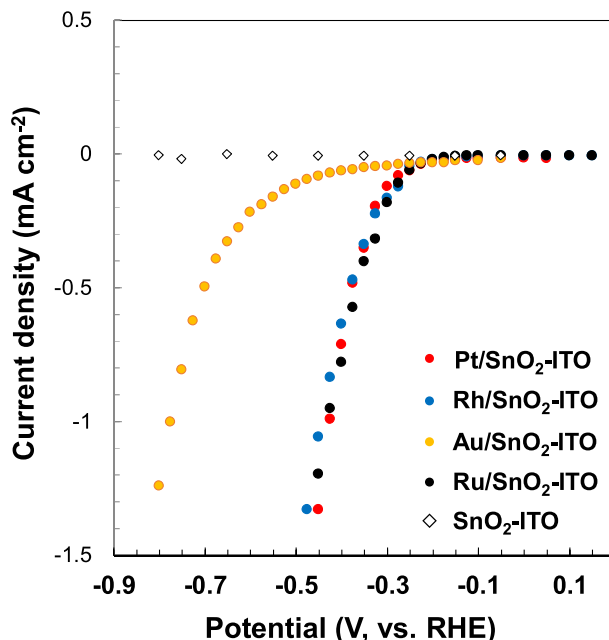**Fig. 7.** Current-voltage plot of various metals (Pt, Rh, Au and Ru, nominal thickness of 1 nm) sputtered on transparent conductive oxide film (SnO$_2$-ITO). These data were obtained from current-time properties measured at each potential in 0.2 M K$_2$SO$_4$ aqueous solution purged with Ar gas using a Ag/AgCl reference electrode and a Pt wire counter electrode.

exhibit correspondingly low IPCE values, future improvements in the crystallinity of these films should allow them to function as photocathodes with exceptional abilities to promote photoreduction generating H$_2$ and hydrocarbons.

4.4. Difference in photocatalytic activities among cocatalyst-loaded Ta-based semiconductors

In a previous report concerning TaON, Ru was shown to be an extraordinarily effective cocatalyst and exhibited a remarkably high H$_2$ evolution rate under visible light irradiation in an aqueous 80 vol% methanol solution, while other noble metals such as Pt, Rh and Ir were not effective for H$_2$ evolution [11]. However, the mechanism of the positive effect of Ru on TaON has not been clarified yet. The same discrepancy is also seen with Ta$_3$N$_5$ [30,31]. These previously reported results are therefore completely different from the data presented herein for N-Ta$_2$O$_5$, even though both semiconductors contain the identical elements. Although it is very difficult to understand the difference in mechanism of N-Ta$_2$O$_5$, TaON and Ta$_3$N$_5$ loaded with metals, the present results could represent a good starting point for the investigation of the correlation between photocatalytic reactions and electronic interactions between semiconductors and metallic cocatalysts.

It is considered that crucial factors are as follows: (1) energy difference between conduction band minimum (E$_{CBM}$) of semiconductors and threshold potential for hydrogen evolution over the metal catalysts, (2) band bending in semiconductor electrode (or charge distribution around cocatalysts/semiconductor interface in powder system) correlated with electronic structure at the semiconductor/metal interface which is explained by the classical theory, (3) properties of electron donation to semiconductor powder from sacrificial electron donor molecules or to semiconductor electrode from the backside of photoelectrode.

Firstly, in order to evaluate the factor (1), linear sweep voltammetry (LSV) of metal cocatalysts (Pt, Au, Rh and Ru) which were sputtered onto a transparent conductive oxide film (SnO$_2$-ITO) was measured. The sputtering conditions were same as those deposited
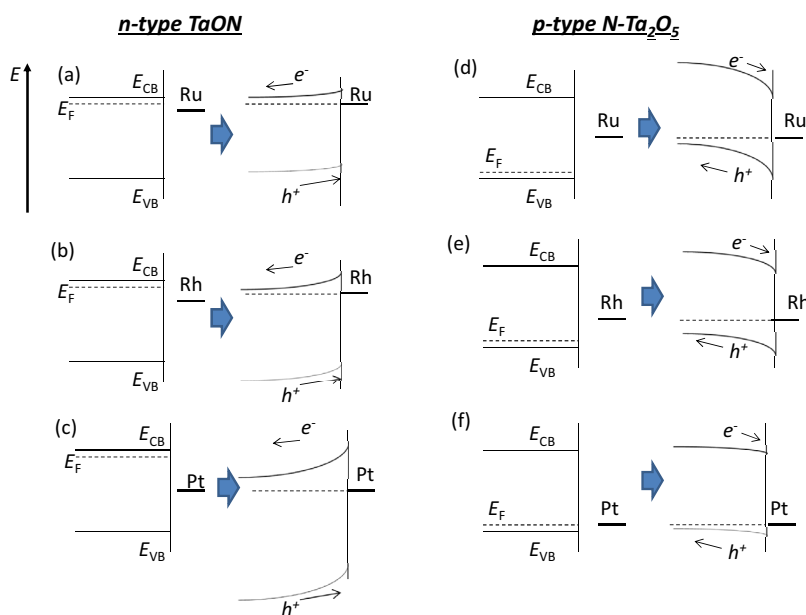
Fig. 8. Proposed schematic illustration of band bending near semiconductor surfaces of N-Ta$_2$O$_5$ and TaON in contact with Ru, Rh and Pt. (a) Ru/TaON, (b) Rh/TaON, (c) Pt/TaON, (d) Ru/N-Ta$_2$O$_5$, (e) Rh/N-Ta$_2$O$_5$ and (f) Pt/N-Ta$_2$O$_5$.

onto N-Ta$_2$O$_5$, and then nominal thickness of them was fixed at 1 nm. The LSV profile was measured in 0.2 M K$_2$SO$_4$ aqueous solution purged with Ar gas. Because Rh, Pt and Au metals showed self-redox current in LSV (Fig. S7), we also measured current-time profiles to determine H$_2$ generation current at each applied potential as shown in Fig. 7. Accordingly, it was revealed that overpotentials for H$_2$ evolution were in the following order: Ru, Pt, Rh (−0.32 V, *vs.* RHE) < Au (−0.65 V). The overpotential of Au was high, while those of Ru, Pt, and Rh were lower and at the same level. It was also confirmed by the Tafel slopes that slopes of Pt, Rh, Ru and Au was determined to be 128, 121, 111 and 389 mV dec^{-1}, respectively (Fig. S8). Therefore H$_2$ generation activity of Au was much lower than Ru, Pt, and Rh.

In Figs. 2 and 7, overlap of E$_{CBM}$ and threshold potential for H$_2$ generation suggests that transfer of conduction band electrons to Au catalyst is more difficult than the cases of Rh, Pt, and Ru, because overpotential for H$_2$ generation over Au catalyst is very high. In fact, enhancement of H$_2$ generation rate by Au deposition on N-Ta$_2$O$_5$ is low as shown in Fig. 4. In the cases of Rh and Pt −loaded N-Ta$_2$O$_5$, H$_2$ generation rates were higher because the overpotential is much lower than that of Au in which electron transfer can be facilitated. In contrast to the case of N-Ta$_2$O$_5$, only Ru showed high activity at TaON [11], though the mechanism has not been unveiled.

Then, we take factor (2) into consideration that the lower activity of Pt and Rh than that of Ru on TaON is correlated with difference in work functions of the metal cocatalysts. In general, the work function of Ru, Rh and Pt are 4.7, 5.0 and 5.6 eV, respectively [32]. In accordance with the classical theory of metal/semiconductor contact, aspect of band bending in semiconductor is dependent of combinations of semiconductors and metals [33]. Fermi levels of *n*-type TaON and *p*-type N-Ta$_2$O$_5$ were estimated to be 4.4 and 5.7 V from reference [6] and Mott-Schottky plot (Fig. S4), respectively. Therefore speculated band banding near semiconductor/metal interfaces after equilibrium can be theoretically illustrated quantitatively in Fig. 8. These diagrams suggest that electron transfer from N-Ta$_2$O$_5$ to the Pt, Rh and Ru cocatalysts is easier, while that from TaON is more difficult. It should also be noted that upward and downward band bending toward the surface also takes place by charge equilibrium between *n*-type and

p-type semiconductor surface and aqueous solution, respectively [34]. However, it is also important to understand the fact that H$_2$ generation was realized even though upward bending was speculated for TaON. A similar example, in a Pt/GaN system, Fermi level shift of Pt particles was observed by FTIR upon irradiation due to electron transfer (*i.e.* increase in electron density in Pt) irrespective of upward bend bending, which is the discrepancy between the theory and the experimental fact of cocatalyst for hydrogen evolution [35].

Furthermore, to understand the discrepancy as mentioned above, we have to take into account the electron donation to semiconductors for the overall reaction, which are oxidation of electron donor molecule and H$_2$ production by proton reduction [factor (3)]. TaON and Ta$_3$N$_5$ powders were prepared for understanding correlation between electron donor and cocatalyst. The reason why we employed powders was that it was very difficult to synthesize TaON and Ta$_3$N$_5$ films by sputtering method. First, we evaluated photocatalytic hydrogen evolution activity in 80 vol% methanol aqueous solution as reported [11] and 100 mM EDTA aqueous solution as shown in Table 3. EDTA is recognized as an effective and irreversible electron donor to enzymes, molecules, and semiconductors. In 80 vol% methanol aqueous solution, Ru-loaded TaON exhibited excellent photocatalytic activity compared with Pt-loaded TaON as reported previously [11]. To the contrary, in aqueous solution with lower concentration of 100 mM EDTA, Pt-loaded TaON drastically improved the activity, while Ru-loaded TaON did not. It was also confirmed that small amount of Ru (0.08) was effective for H$_2$ generation, while 0.39%-Ru was not, which was consistent with the previous report suggesting high activity at only low amount of Ru [11]. Pt-loaded N-Ta$_2$O$_5$, Pt-loaded TaON and Pt-loaded Ta$_3$N$_5$ in solution containing 100 mM EDTA also showed great enhancement in activity compared to the case in methanol electron donor. Here, it is widely accepted that EDTA is one of very effective electron donor. Therefore, these results indicate that electron donating activity of molecular sacrificial reagent is crucial to discuss H$_2$ generation activity in the metal-loaded Ta-based semiconductor photocatalysis. In the present case, we also confirmed that pH difference between methanol (pH 7.0) and EDTA (4.4) system is not the main cause for difference in H$_2$ generation rate.
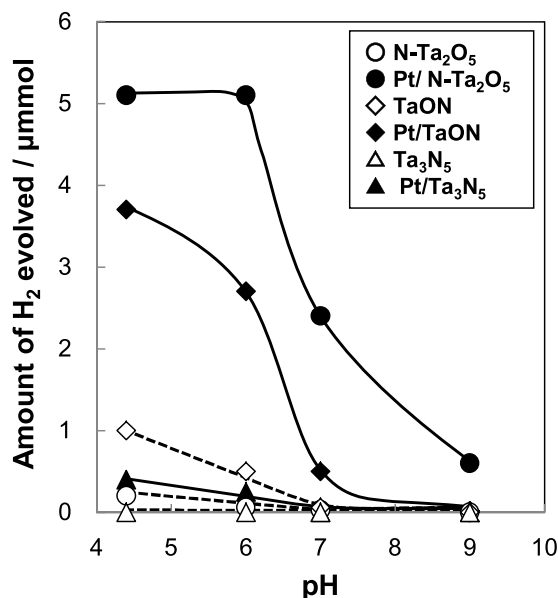
Fig. 9. pH dependence of photocatalytic activities for H_2 evolution using Pt-loaded N-Ta_2O_5, TaON and Ta_3N_5 particles (8 mg catalyst) in 4 ml Ar-saturated 100 mM EDTA aqueous solution measured under visible light irradiation ($410 \leq \lambda \leq 750$ nm, 24 h).

Here, the pH dependence of photocatalytic activities for H_2 evolution of various Pt-loaded Ta-based semiconductors in 100 mM EDTA aqueous solution under visible solution was also evaluated. In Fig. 9, Pt loaded N-Ta_2O_5 showed highest activity at pH 4.4 and 6, and maintained activity even at pH 7 and 9. In contrast, TaON and Ta_3N_5 showed very low activity at pH 7, and almost no activity at pH 9. Because the hydrogen evolution potential shift negatively with increasing pH ($E(V)$ *vs.* NHE = −0.059 pH), it is difficult to induce proton reduction of TaON and Ta_3N_5 at neutral pH and above. However, Pt loaded N-Ta_2O_5 catalyst with much negative position of E_{CBM} catalyzed hydrogen generation. These results indicate that *p*-type N-Ta_2O_5 is applicable in wider pH range for visible-light driven photocatalysis.

These (1)–(3) items could explain that photocatalytic H_2 production in aqueous solution is basically determined by energy difference between E_{CBM} of semiconductors and threshold potential for hydrogen evolution over the metal catalysts. Additionally, band bending correlated with electronic structure at the semiconductor/metal interface and properties of electron donation from the sacrificial donor or electrode backside dominates the reaction rates and selection of cocatalysts. These fundamental researches on this topic could also be an essential factor for optimizing electronic interactions between cocatalysts and semiconductors.

5. Conclusions

The N doping into Ta_2O_5 induced a redshift in the optical absorption edge from 320 to 500 nm, resulting in the absorption of visible light. Simultaneously, the N doping caused a change in the conduction from *n*-type to *p*-type, resulting in a cathodic photoresponse. The N-Ta_2O_5 photocathode has a highly negative E_{CBM} potential than conventional Ta_2O_5 or TaON, which is induced by strong charge localization at the surface. We have demonstrated H_2 evolution over N-Ta_2O_5 by water splitting in aqueous solution under visible light irradiation. The rate of H_2 generation was greatly enhanced by loading with Pt, Rh or Au as cocatalysts. At this moment, the conversion efficiency was low as 0.15% at 400 nm. However, the dual functional modification of Ta_2O_5 by the single element doping of N was clarified to be as a new approach to

facilitate the reductive reaction for energy conversion. This finding should assist in the future development of highly efficient photocatalysts for solar energy conversion by photoelectrochemistry by N doping into oxide semiconductor materials.

Appendix A. Supplementary data

Supplementary data associated with this article can be found, in the online version, at http://dx.doi.org/10.1016/j.apcatb.2016.09.066.

References

[1] T. Morikawa, S. Saeki, T. Suzuki, T. Kajino, T. Motohiro, Appl. Phys. Lett. 96 (2010) 142111.
[2] T.M. Suzuki, T. Nakamura, S. Saeki, Y. Matsuoka, H. Tanaka, K. Yano, T. Kajino, T. Morikawa, J. Mater. Chem. 22 (2012) 24584.
[3] K. Sayama, H. Arakawa, J. Photochem. Photobiol. A 77 (1994) 243.
[4] H. Kato, A. Kudo, Chem. Phys. Lett. 295 (1998) 487.
[5] Y. Takahara, J.N. Kondo, T. Takata, D. Lu, K. Domen, Chem. Mater. 13 (2001) 1194.
[6] W.-A. Chun, A. Ishikawa, H. Fujisawa, T. Takata, J.N. Kondo, M. Hara, M. Kawai, Y. Matsumoto, K. Domen, J. Phys. Chem. B 107 (2003) 1798.
[7] S. Sato, T. Morikawa, S. Saeki, T. Kajino, T. Motohiro, Angew. Chem. Int. Ed. 49 (2010) 5101.
[8] T.M. Suzuki, H. Tanaka, T. Morikawa, M. Iwaki, S. Sato, S. Saeki, M. Inoue, T. Kajino, T. Motohiro, Chem. Commun. 47 (2011) 8673.
[9] K. Yamanaka, S. Sato, M. Iwaki, T. Kajino, T. Morikawa, J. Phys. Chem. C 115 (2011) 18348.
[10] A.V. Akimov, R. Jinnouchi, S. Shirai, R. Asahi, O.V. Prezhdo, J. Phys. Chem. B 119 (2015) 7186.
[11] M. Hara, T. Kondo, M. Komoda, S. Ikeda, K. Shinohara, A. Tanaka, J.N. Kondo, K. Domen, Chem. Commun. (1998) 357.
[12] J.-N. Nian, C.-C. Hu, H. Teng, Int. J. Hydrogen Energy 33 (2008) 2897.
[13] C.G. Read, Y. Park, K.-S. Choi, J. Phys. Chem. Lett. 3 (2012) 1872.
[14] K. Iwashina, A. Kudo, J. Am. Chem. Soc. 133 (2011) 13272.
[15] C. Leygraf, M. Hendewerk, G.A. Somorjai, J. Phys. Chem. 86 (1982) 4484.
[16] W.B. Ingler, Jr., J.P. Baltrus, S.U.M. Khan, J. Am. Chem. Soc. 126 (2004) 10328.
[17] T. Morikawa, K. Kitazumi, N. Takahashi, T. Arai, T. Kajino, Appl. Phys. Lett. 98 (2011) 242108.
[18] T. Morikawa, T. Arai, T. Motohiro, Appl. Phys. Express 6 (2013) 041201.
[19] Y. Matsumoto, M. Obata, J. Hombo, J. Phys. Chem. 98 (1994) 2950.
[20] S. Ida, K. Yamada, T. Matsunaga, H. Hagiwara, Y. Matsumoto, T. Ishihara, J. Am. Chem. Soc. 132 (2010) 17343.
[21] K. Sekizawa, T. Nonaka, T. Arai, T. Morikawa, ACS Appl. Mater. Interfaces 6 (2014) 10969.
[22] T.M. Suzuki, G. Kitahara, T. Arai, Y. Matsuoka, T. Morikawa, Chem. Commun. 50 (2014) 7614.
[23] R. Asahi, T. Morikawa, Chem. Phys. 339 (2007) 57.
[24] R. Asahi, T. Morikawa, H. Irie, T. Ohwaki, Chem. Rev. 19 (2014) 114.
[25] A. Tsukazaki, A. Ohtomo, T. Onuma, M. Ohtani, T. Makino, M. Sumiya, K. Ohtani, S.F. Chichibu, S. Fuke, Y. Segawa, H. Ohno, H. Koinuma, M. Kawasaki, Nat. Mater. 4 (2005) 42.
[26] Y. Nakano, T. Morikawa, T. Ohwaki, Y. Taga, Appl. Phys. Lett. 88 (2006) 172103.
[27] R. Jinnouchi, A.V. Akimov, S. Shirai, R. Asahi, O.V. Prezhdo, J. Phys. Chem. C 119 (2015) 26925.
[28] S. Sato, T. Arai, T. Morikawa, K. Uemura, T.M. Suzuki, H. Tanaka, T. Kajino, J. Am. Chem. Soc. 133 (2011) 15240.
[29] M. Hara, J. Nunoshige, T. Takata, J.N. Kondo, K. Domen, Chem. Commun. (2003) 3000.
[30] G. Hitoki, A. Ishikawa, T. Takata, J.N. Kondo, M. Hara, K. Domen, Chem. Lett. 7 (2002) 736.
[31] M. Hara, G. Hitoki, T. Takata, J.N. Kondo, H. Kobayashi, K. Domen, Catal. Today 78 (2003) 555.
[32] H.B. Michaelson, J. Appl. Phys. 48 (1977) 4729.
[33] Z. Zhang, J.T. Yates Jr., Chem. Rev. 112 (2012) 5520.
[34] M.G. Walter, E.L. Warren, J.R. McKone, S.W. Boettcher, Q. Mi, E.A. Santori, N.S. Lewis, Chem. Rev. 110 (2010) 6446.
[35] M. Yoshida, A. Yamakata, K. Takanabe, J. Kubota, M. Osawa, K. Domen, J. Am. Chem. Soc. 131 (2009) 13218.